Electronic Supplementary Material (ESI) for ChemComm.

Supporting information

High Turnover Photocatalytic Hydrogen Formation with an Fe(III) *N*-Heterocyclic Carbene Photosensitizer

Jesper Schwarz[‡a], Aleksandra Ilic[‡a], Catherine Johnson[‡b], Reiner Lomoth*[b] and Kenneth Wärnmark*[a]

[a]Center for Analysis and Synthesis (CAS), Department of Chemistry, Lund University, SE-22100 Lund, Sweden;
[b]Department of Chemistry–Ångström Laboratory, Uppsala University, SE-75120 Uppsala, Sweden.

‡These authors contributed equally.

***Corresponding Author**

E-mail: reiner.lomoth@kemi.uu.se
E-mail: kenneth.warnmark@chem.lu.se

Table of Contents

General Information

Materials and Instruments

Materials. All solvents used were obtained from commercial suppliers and used without further purification. Reagents *i.e.,* K_2PtCl_4, sacrificial reductants and dimethylglyoxime were purchased from Sigma-Aldrich and used without further purification. $[Fe(phtmeimb)_2]PF_6$,[1] $[Co(dmgH)_2pyCl]$[2], $[HNEt_3][BF_4]$[3] and *p*-cyanoanilinium tetrafluoroborate[3] were prepared according to literature procedures.

Photoreactions. Generally, photoreactions were performed in a TAK120 AC photoreactor purchased from HK Testsysteme GmBH. The irradiation was performed using the green LED array (λ=530 nm, 3.15 W/vial) unless otherwise stated. All HERs were run in 4.9 mL clear glass vials with screw caps with a PTFE/silicone septum and degassed by bubbling with Ar (g) before irradiation. The temperature during reaction was maintained at 28–32 °C using air cooling.

Hydrogen quantification. The amount of hydrogen in the headspace was determined using a custom-built Raman based spectrometer. This was calibrated against a hydrogen microsensor (H_2-NP) connected to a UniAmp Multi Channel x-5 amplifier, both from Unisense A/S. For recording and calibration of the microsensor the SensorTrace suite, also from Unisense, was used. For calibration curves comparing the Raman spectrometer with the microsensor see section "H_2 calibration curves" below. The amount of hydrogen dissolved in the solvent was deemed to be very minor compared to the amount in the headspace.[4]

UV-vis spectroscopy. UV-Vis absorption spectra were recorded on Varian Cary 50 Spectrophotometer and a Probe Drum Lab-in-a-box spectrometer.

Emission measurements. Steady-state emission measurements (excitation wavelength 502 nm) were performed on FS5 (Edinburgh Instruments) or Fluorolog-3 (Horiba) fluorimeters with slit widths set to 4 nm spectral resolution. Emission spectra from both instruments were background subtracted and corrected for the wavelength dependent instrument response. Solutions of $[Fe(phtmeimb)_2]PF_6$ were prepared in acetonitrile (spectroscopic grade Uvasol®, ≥99.9%, from Merck) with absorption of around 0.05 ± 0.005 at 502 nm. UV-Vis absorption and two emission spectra were taken for each quencher concentration and emission intensities were corrected for minor differences in absorbance at the excitation wavelength. In addition, background emission measurements for just the quencher at the same concentrations were measured. Stern-Volmer plots were constructed from the emission intensities taken at 650 nm from the averaged and background subtracted spectra and fitted with Origin software. Emission lifetimes were determined by TCSPC performed with the FS5 (Edinburgh Instruments) fluorimeter. Emission decays at 650 nm were recorded with slit width of 8 nm and counts of around 65,000. The instrument response function (IRF) was collected with a scattering sample (LUDOX). The kinetic decays were fitted along with the IRF using the in-built software.

Nanosecond transient absorption measurements. Nanosecond transient absorption measurements were obtained with a LP920-S laser flash photolysis spectrometer (Edinburgh Instruments) equipped with an iStar CCD camera (Andor Technology) for transient spectra and a LP920-K PMT detector connected to a TDS 3052 500 MHz 5 GS/s oscilloscope (Tektronix) for single wavelength kinetics. Probe light was provided by a pulsed XBO 450 W

Xenon Arc Lamp (Osram) and samples were excited at 465 nm with 8 ns pulses (18.9 ± 0.3 mJ/pulse) provided by a frequency tripled Q-switched Nd:YAG laser (EKSPLA NT342B) combined with an optical parametric oscillator (OPO). All measurements were performed at right angle in a 10 × 10 mm quartz cuvette with samples deaerated by purging with Ar and an absorption of around 0.5 at the excitation wavelength. Quencher concentrations were 316.22 mM (TEOA) or 14.86 mM ($Co(dmgH)_2pyCl$).

HER Experimental Details

Optimization of Pt-catalyzed HER

Typical experimental conditions in the optimization of the Pt-catalyzed HER were: $[Fe(phtmeimb)_2]PF_6$[1] (see [PS] column), K_2PtCl_4 (see [PRC] column), $[HNEt_3][BF_4]$[3] (165 mM) and Et_3N (0.500 M) in acetonitrile (total volume 2 mL) was degassed by bubbling with Ar (g) and irradiated with green LEDs (λ = 530 nm, 3.15 W) in a 4.9 mL septum lid vial at 28-32 °C. The amount of hydrogen in the headspace was measured at regular time intervals by Raman spectroscopy.

Table S1. HER using $[Fe(phtmeimb)_2]PF_6$ as PS, K_2PtCl_4 as PRC, $[HNEt_3][BF_4]$ as proton source, and Et_3N as SR.

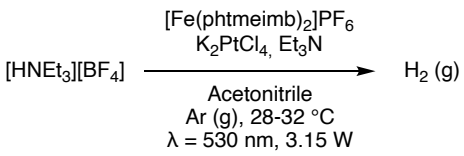

Entry	[PS] (mM)	[PRC] (mM)	Time (h)	H_2 (μmol)	TON[a]
1[b]	1	0.45	21	48.0	53.3
2	2	0.45	21	36.5	40.5
3	0.5	0.45	21	15.6	17.4
4[b]	-	0.2	17	n.d.[c]	-
5[d]	1	-	17	1.96	0.98[e]

[a]TON = mol of H_2 / mol of PRC. [b]average of 2 replicates [c]n.d. = no hydrogen detected. [d]average of 4 replicates [e]TON = mol of H_2 / mol of PS.

Table S2. Optimization of the amount of K_2PtCl_4 in the HER using $[Fe(phtmeimb)_2]PF_6$ as PS and $[HNEt_3][BF_4]$ as the proton source.

Entry	[PRC] (mM)	Time (h)	H_2 (μmol)	TON	Initial TOF (h^{-1})
1	0.9	21	5.79	3.22	
2[a]	0.2	17	53.7	134	
3[b]	0.1	17	56.4	282	
4	0.05	22	117.6	1176	65
5	0.01	20	12.2	612	68
6[a]	0.005	17	7.12	712	

[PS] = 1 mM [a]average of 2 replicates. [b]average of 3 replicates

Table S3. Variation of sacrificial reductant and proton source in the HER using $[Fe(phtmeimb)_2]PF_6$ as PS and K_2PtCl_4 as the PRC.

Entry	Reductant	Proton source	[PRC] (mM)	H_2 (µmol)	TON
1[a]	TEOA	$[HNEt_3][BF_4]$	0.2	71.4	179
2[a]	TEOA	$[HNEt_3][BF_4]$	0.05	13.7	137
3[a]	TEOA	$[HNEt_3][BF_4]$	0.01	2.3	115
4[a]	TEOA	$[HNEt_3][BF_4]$	-	0.72	0.4
5[a]	Et_3N	*p*-CN-anilinium[b]	0.2	59.3	148
6[a]	Na-ascorbate[c]	$[HNEt_3][BF_4]$	0.2	n.d.[d]	-

[PS] = 1 mM, Reaction time: 17 h. [a]average of 2 replicates. [b]*p*-cyanoanilinium tetrafluoroborate. [c]Na-ascorbate was poorly soluble in the solvent. [d]n.d. = no hydrogen detected.

Optimization of Co-catalyzed HER

Table S4. Variation of PS- and PRC-concentrations for the $[Co(dmgH)_2pyCl]$ catalyzed HER.

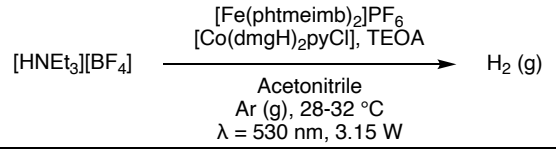

Entry	[PS] (mM)	[PRC] (mM)	$[H^+]$[a] (mM)	Time (h)	H_2 (µmol)	TON
1	0.1	0.5	66	18	33	33
2[a]	0.1	0.5	66[a]	22	23	22
3	0.1	0.1	165	6	7.4	37
4	0.5	0.1	165	4	9	45
5	1	0.1	165	6	10	49

[a]Concentration of the proton source $[HNEt_3][BF_4]$ [b]proton source = *p*-cyanoanilinium tetrafluoroborate. [TEOA] = 377 mM.

Table S5. Variation of sacrificial reductant concentration for the $[Co(dmgH)_2pyCl]$ catalyzed HER.

Entry	SR	[SR] (M)	H_2 (µmol)	TON
1	TEOA	2	1.8	7
2	TEOA	1	3.1	14
3	TEOA	0.25	7.5	37
4	Et_3N	0.5	1	5

[PS] = 0.5 mM, [PRC] = 0.1 mM, $[HNEt_3][BF_4]$ = 165 mM in acetonitrile. SR = Sacrificial reductant, Reaction time: 6 h.

Table S6. Variation of reaction solvent for the $[Co(dmgH)_2pyCl]$ catalyzed HER.

Entry	Solvent	Time (h)	H_2 (µmol)	TON
1	MeCN	4	9	45
2	Acetone	18	1.2	6
3	DCM	18	n.d.[a]	-
4	MeOH	18	5.1	25
5	DMSO	18	n.d.[a]	-

[PS] = 0.5 mM, [PRC] = 0.1 mM, $[HNEt_3][BF_4]$ = 165 mM, [TEOA]= 377 mM in acetonitrile. [a]n.d. = no hydrogen detected.

Table S7. Variation of PS- and PRC-concentrations for the [Co(dmgH)$_2$pyCl] catalyzed HER in presence of different amounts of added free ligand.

Entry	[PS] (mM)	[PRC] (mM)	[dmgH$_2$] (mM)	Time (h)	H$_2$ (µmol)	TON	Initial TOF (h^{-1})
1[a]	0.5	0.1	3	17	100	498	-
2	0.5	0.05	3	22	93	927	63
3[b]	0.5	0.05	3	21	69	688	39
4	0.5	0.01	3	21	21	1024	152
5	0.5	0.005	3	21	13	1311	152
5	0.75	0.05	3	20	90	900	53
6	1	0.05	3	20	80	800	49
7	0.5	0.05	1	20	53	532	60
8	0.5	0.05	3	22	113	1132	65
9	0.5	0.05	5	22	120	1199	60
10	0.5	0.05	10	22	109	1090	53

[HNEt$_3$][BF$_4$] = 165 mM, [TEOA] = 377 mM in acetonitrile. [a][HNEt$_3$][BF$_4$] = 66 mM. [b]pH adjusted to 6.92 using HBF$_4$·Et$_2$O.

Control Experiments

Table S8. HER using [Co(dmgH)$_2$pyCl] or Pt-colloids (Pt) as PRC and [Fe(phtmeimb)$_2$]PF$_6$ as PS without added proton source and with added water.

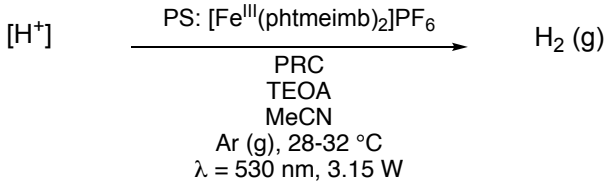

Entry	PRC	[H$_2$O] (% v/v)	Time (h)	H$_2$ (µmol)	TON
1[a]	[Co(dmgH)$_2$pyCl]	-	19	8	40
2	[Co(dmgH)$_2$pyCl]	-	19	39	188
3[b]	[Co(dmgH)$_2$pyCl]	50	24	n.d.	-
4	[Co(dmgH)$_2$pyCl]	10	20	7.6	38
5	[Co(dmgH)$_2$pyCl]	5	6	13	63
6	[Co(dmgH)$_2$pyCl]	5	20	20	102
7	[Co(dmgH)$_2$pyCl]	2.5	20	38	190
8	[Co(dmgH)$_2$pyCl]	1.25	20	37	185
9[c]	Pt	-	19	n.d.[e]	-
10	Pt	-	19	29	33
11[c,d]	Pt	20	24	n.d.	-
12	Pt	2.5	20	21	46
13[c]	Pt	5	22	n.d.	-

Reaction conditions for [Co(dmgH)$_2$pyCl]: 0.5 mM PS, 0.1 mM PRC, 0.377 M TEOA, 3 mM dmgH$_2$ & H$_2$O in acetonitrile. Reaction conditions for Pt: 1 mM PS, 0.45 mM PRC, 0.5 M TEOA & H$_2$O in acetonitrile. [a] without added dmgH$_2$, [b] adjusted pH = 7.02, [c] Et$_3$N as sacrificial reductant. [d] 0.45 mM PRC. [e]n.d. = no hydrogen detected.

Table S9. Control reactions with other Iron PS using K_2PtCl_4 and $[Co(dmgH)_2pyCl]$ as catalyst precursors. All reactions are duplicates. L = bis(2,6-bis(3-methylimidazol-1-ylidene)pyridine), $[Et_3N]$ = 0.5 M, [Proton source] = 165 mM. n.d = no hydrogen detected.

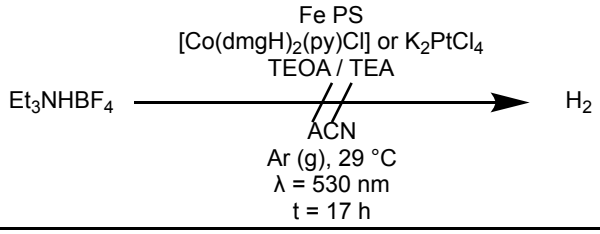

Entry	PS	[PS] (mM)	PRC	[PRC] (mM)	Wavelength (nm)	Proton source	Time (h)	H_2 (µmol)
1	$[FeL_2](PF_6)_2$	1	K_2PtCl_4	0.45	530	$[HNEt_3][BF_4]$	20	n.d.
2	$[FeL_2](PF_6)_2$	0.5	$[Co(dmgH)_2(py)Cl]$	0.1	530	$[HNEt_3][BF_4]$	20	n.d.
3	$[FeL_2](PF_6)_2$	0.5	$[Co(dmgH)_2(py)Cl]$	0.1	455	$[HNEt_3][BF_4]$	21	n.d.
4	$[Fe(bpy)_3](PF_6)_2$	1	K_2PtCl_4	0.2	530	$[HNEt_3][BF_4]$	17	n.d.
5	$[Fe(bpy)_3](PF_6)_2$	0.5	$[Co(dmgH)_2(py)Cl]$	0.1	530	$[HNEt_3][BF_4]$	17	n.d.
6	$[FeL_2](PF_6)_2$	1	K_2PtCl_4	0.45	455	20 % H_2O	20	n.d.
7	$[FeL_2](PF_6)_2$	1	K_2PtCl_4	0.45	455	*p*-CN-anilinium (BF_4)	20	n.d.

n.d. = no hydrogen detected.

Time Trace for $[Ru(bpy)_3]^{2+}$ and Pt-colloid

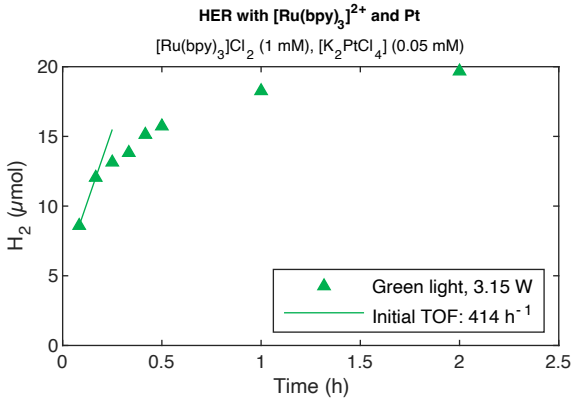

Figure S1. Time trace of HER using $[Ru(bpy)_3]Cl_2$ (1 mM), K_2PtCl_4 (0.05 mM), $[HNEt_3][BF_4]$ (165 mM), Et_3N (500 mM) in acetonitrile at 3.15 W light intensity (λ = 530 nm).

UV-vis absorption spectra

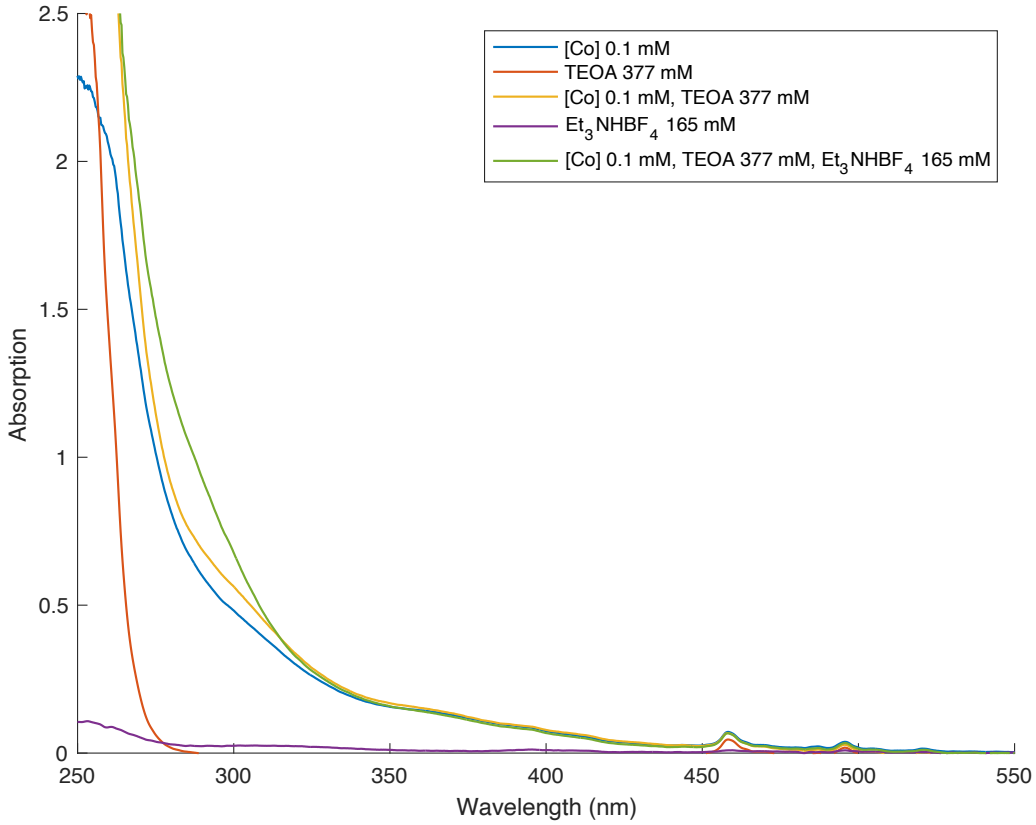

Figure S2. UV-vis absorption spectra of $[Co(dmgH)_2pyCl]$, TEOA, $[HNEt_3][BF_4]$ and mixtures thereof.

Quantum Yield Measurements

The quantum yields for the HER using [Co(dmgH)$_2$pyCl] and Pt-colloids as PRC and [Fe(phtmeimb)$_2$]PF$_6$ as PS were determined using a method developed by Pitre *et al.*[6], wherein the oxidation of 9,10-diphenylanthracene (DPA) catalysed by [Ru(bpy)$_3$]Cl$_2$ in acetonitrile was used to quantify the number of moles of photons absorbed by the sample.

All samples were irradiated for 3 min in the same slot at 530 nm (3.15 W/slot) in a TAK120 AC photoreactor purchased from HK Testsysteme GmBH. For irradiation 4.9 mL glass vials with screw caps were used. UV-vis absorption measurements were performed on a Probe Drum Lab-in-a-box spectrometer and samples were contained in a 10 mm quartz cuvette.

A reaction solution (2 mL) with 0.6 mM [Ru(bpy)$_3$]Cl$_2$·6 H$_2$O and 0.1 mM DPA in acetonitrile was irradiated for 3 min. All reaction solutions were prepared under exclusion of light and samples for UV-vis spectroscopy were stored in amber glass vials before transferring to the cuvette. Due to the comparatively low absorptivity of [Ru(bpy)$_3$]Cl$_2$·6 H$_2$O at 530 nm, its concentration was not adapted to match the absorbance of the Fe-PS in the reaction system. Instead, a correction factor was introduced to account for the difference in incident photon absorption.

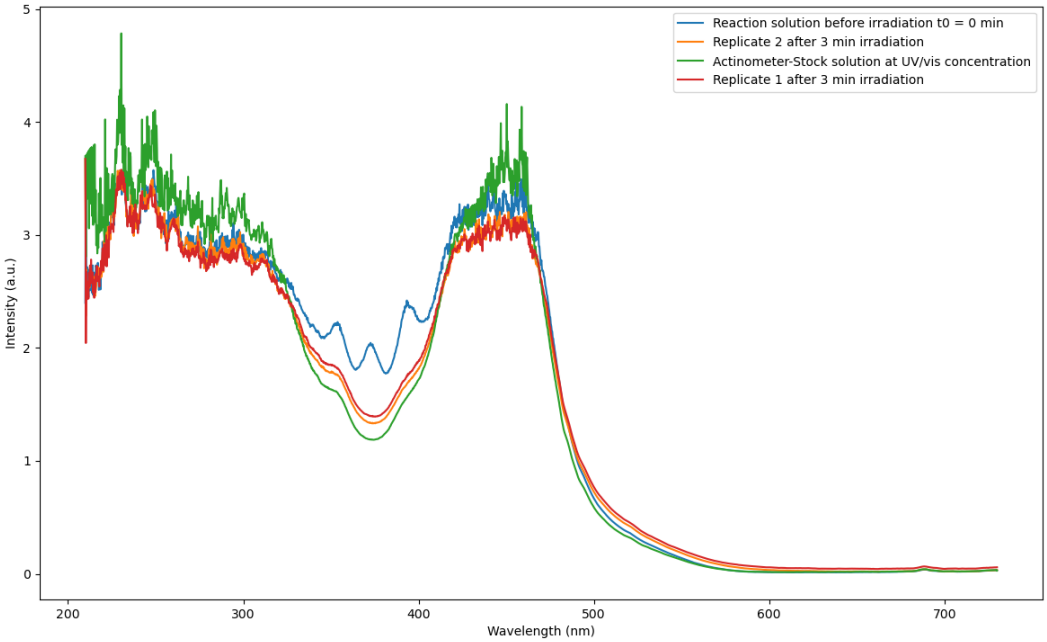

Figure S3: Absorption spectra for the oxidation of DPA using [Ru(bpy)$_3$]Cl$_2$·6 H$_2$O

The calculations were done following the procedure described in the reference manual and gave the results afforded in **S12**.

$$\text{n (mol of DPA consumed)} = \left(\frac{A_{\text{initial}} - A_{\text{final}}}{\varepsilon_{372\text{ nm}} l}\right) \cdot V \qquad \textbf{(Eq. 1)}$$

$$f = 1 - 10^{-(Abs)} \qquad \textbf{(Eq. 2)}$$

$$\frac{Nh\nu}{t} = \frac{\text{n (moles of DPA consumed)}}{\Phi_{\text{actinometer}} t} \cdot \frac{\text{f(HER reaction)}}{\text{f(Ru - actinometer solution)}} \qquad \textbf{(Eq. 3)}$$

$$\Phi_{H_2} = \frac{\text{n (moles of } H_2 \text{ formed)}}{t} \cdot \left(\frac{Nh\nu}{t}\right)^{-1} \qquad \textbf{(Eq. 4)}$$

- $A_{initial}$…absorbance of the solution at 372 nm before irradiation
- A_{final}…absorbance of the solution at 372 nm after 3 min of irradiation
- $\varepsilon_{372\text{ nm}}$…molar extinction coefficient of DPA at 372 nm in acetonitrile (11100 $M^{-1}cm^{-1}$)
- l…path length of the cuvette (cm)
- V…Volume (L)
- $\frac{Nh\nu}{t}$…moles of absorbed photons by sample per time unit
- $\Phi_{actinometer}$…quantum yield of the actinometer (0.019)
- Φ_{HER}…quantum yield of the HER
- f…fraction of incident photons absorbed = correction factor
- Abs…absorbance at 530 nm

Table S10: Data for the determination of the Quantum Yield for the HER reaction using $[Co(dmgH)_2pyCl]$ and Pt-colloids as PRC respectively. ([a]The amount of H_2 corrected by a factor of 0.26 to account for the differences in sample volume compared to the actinometer reaction.).

HER using $[Co(dmgH)_2pyCl]$ as PRC			
	$A_{initial}$(372 nm)	**A_{final}(372 nm)**	**n (moles of H_2 produced in 60 min)[a]**
Replicate 1	2.024	1.418	1.588E-06
Replicate 2	2.024	1.35	
HER using Pt-colloids as PRC			
	$A_{initial}$(372 nm)	**A_{final}(372 nm)**	**n (moles of H_2 produced in 60 min)[a]**
Replicate 1	2.024	1.418	1,397E-06
Replicate 2	2.024	1.35	

Table S11: Calculation of the correction factors (**Eq. 2**) to account for the different absorbance of $[Ru(bpy)_3]Cl_2$ and $[Fe(phtmeimb)_2]PF_6$ at 530 nm using the concentrations of 0.6 mM Ru-PS as well as 0.5 mM & 1 mM Fe-PS.

	0.6 mM $[Ru(bpy)_3]Cl_2$	**0.5 mM $[Fe(phtmeimb)_2](PF_6)$ (Co-HER)**	**1 mM $[Fe(phtmeimb)_2](PF_6)$ (Pt-HER)**
Abs	0.48	1.562	3.124
f	0.67	0.973	0.999
f(HER)/f(Ru-actinometer)	-	**1.457**	**1.497**

Table S12: Results for the determination of the Quantum Yield for the HER reaction using [Co(dmgH)$_2$pyCl] and Pt-colloids as PRC respectively. ([a]The amount of DPA consumed was determined using **Eq. 1**. Aliquots of 750 µL of the reaction solutions were diluted for UV-vis absorption spectroscopy with a dilution factor of 2.)

	n(DPA consumed) (mol)[a]	**Co-HER: Φ_{H_2}**
Replicate 1	8,19E-08	0.013
Replicate 2	9,11E-08	0.011
	n(DPA consumed) (mol)[a]	**Pt-HER: Φ_{H_2}**
Replicate 1	8,19E-08	0.011
Replicate 2	9,11E-08	0.010

H_2 Calibration Curves

Calibration curves were recorded using a 4.9 mL clear glass vial (the same type used for the HERs). Exact quantities of H_2 were added using gas tight syringes (Hamilton) to the vial previously flushed with Argon. The concentration of H_2 in the headspace was simultaneously recorded using a Raman based spectrometer and a H_2-microsensor from Unisense. For high concentrations of hydrogen (Figure S7), large quantities of hydrogen (up to 5 mL) were added. This meant that the vial was leaking substantially, as the pressure increased. This can be seen in the calibration curve of said measurement, which gave somewhat lower slopes of the calibration curves.

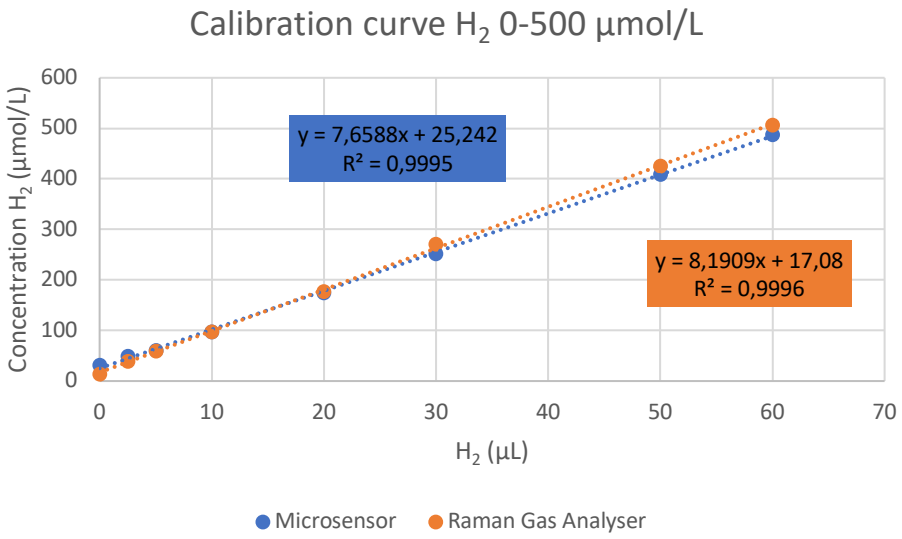

Figure S4. Calibration curve for 0 – 60 µL of hydrogen added to an Ar-flushed 4.9 mL clear glass vial.

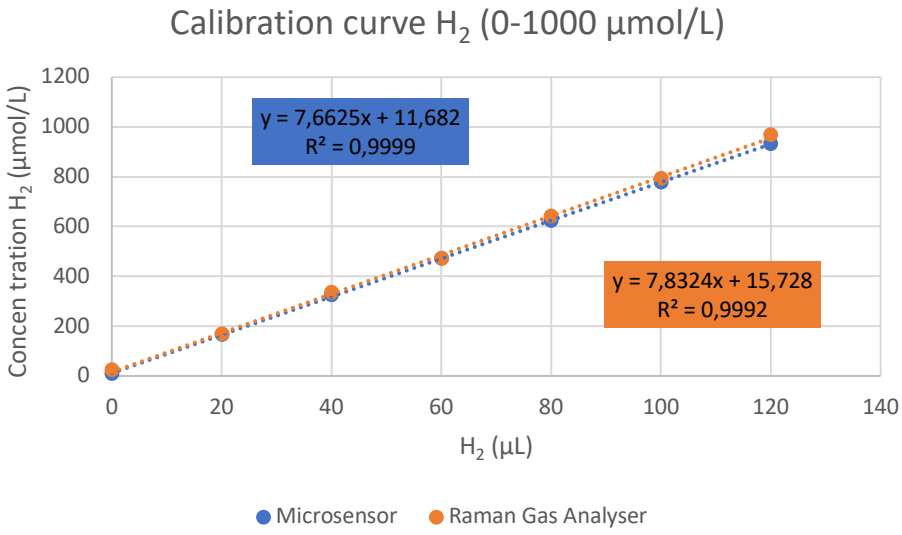

Figure S5. Calibration curve for 0 – 120 µL of hydrogen added to an Ar-flushed 4.9 mL clear glass vial.

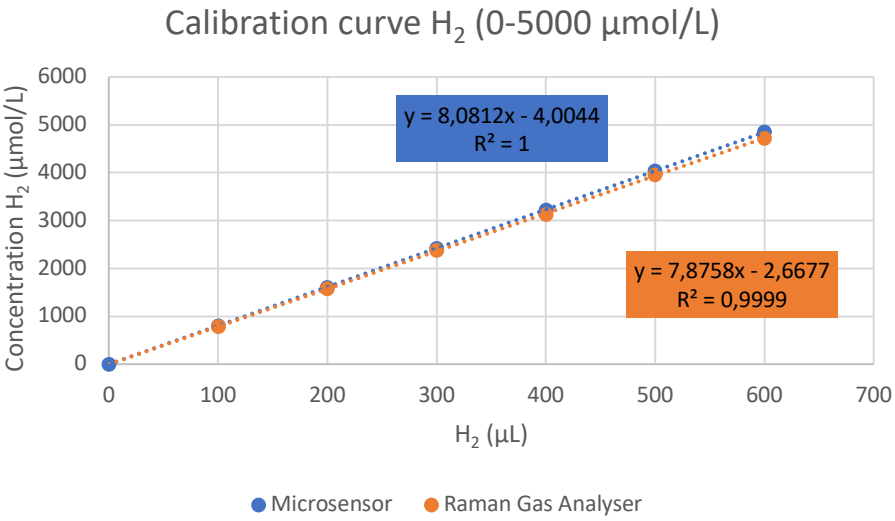

Figure S6. Calibration curve for 0 – 600 µL of hydrogen added to an Ar-flushed 4.9 mL clear glass vial.

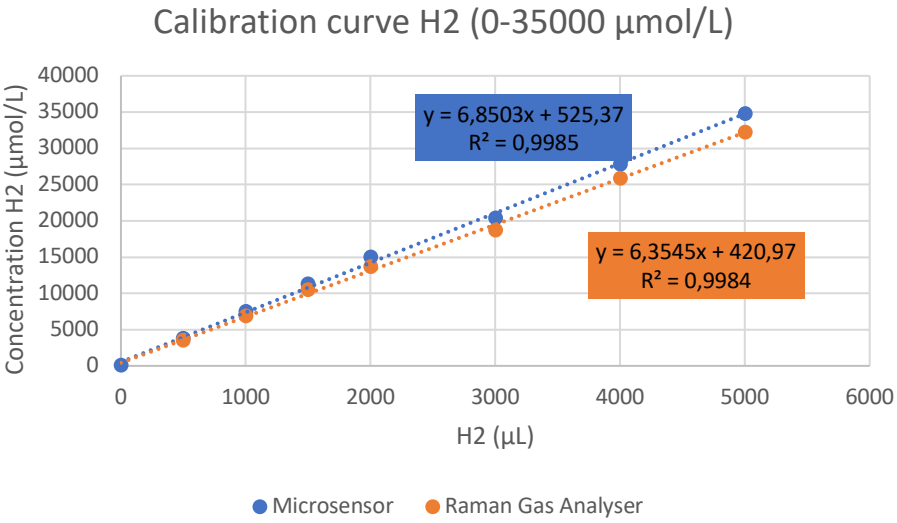

Figure S7. Calibration curve for 0 – 5000 µL of hydrogen added to an Ar-flushed 4.9 mL clear glass vial.

Excited State Quenching

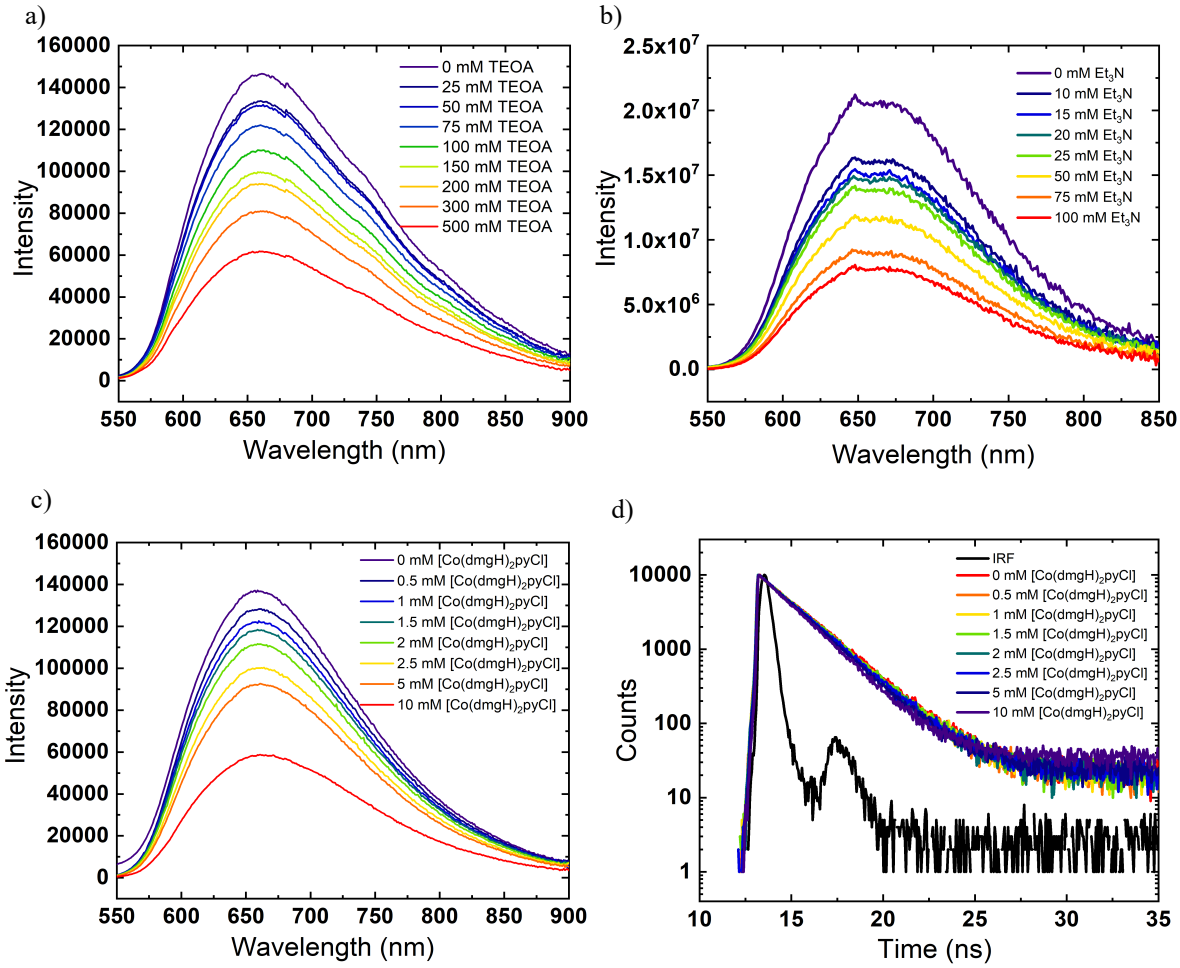

Figure S8. Quenching of $[Fe(phtmeimb)_2]^+$ emission with (a) TEOA, (b) Et_3N, (c,d) $[Co(dmgH)_2pyCl]$.

Reduction of $[Fe(phtmeimb)_2]^{2+}$ by Et_3N and TEOA

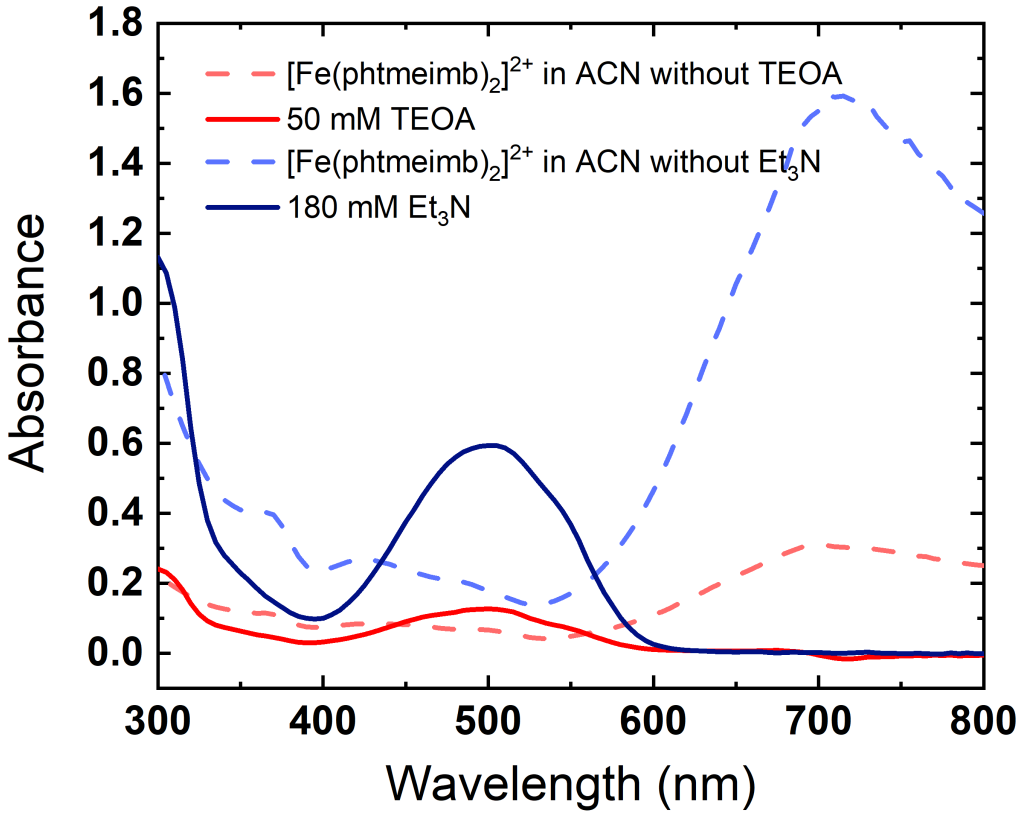

Figure S9. Reduction of $[Fe(phtmeimb)_2]^{2+}$ to $[Fe(phtmeimb)_2]^{+}$. Spectra before and after addition of TEOA (50 mM) or Et_3N(180 mM).

Stability of the PS in the presence of water

The lack of hydrogen formation from water does not seem to originate from instability of $[Fe(phtmeimb)_2]PF_6$ in presence of water, as can be seen from the UV-vis spectrum before and after irradiation (Figure S10). At higher water concentrations the solubility of the PS decreases.

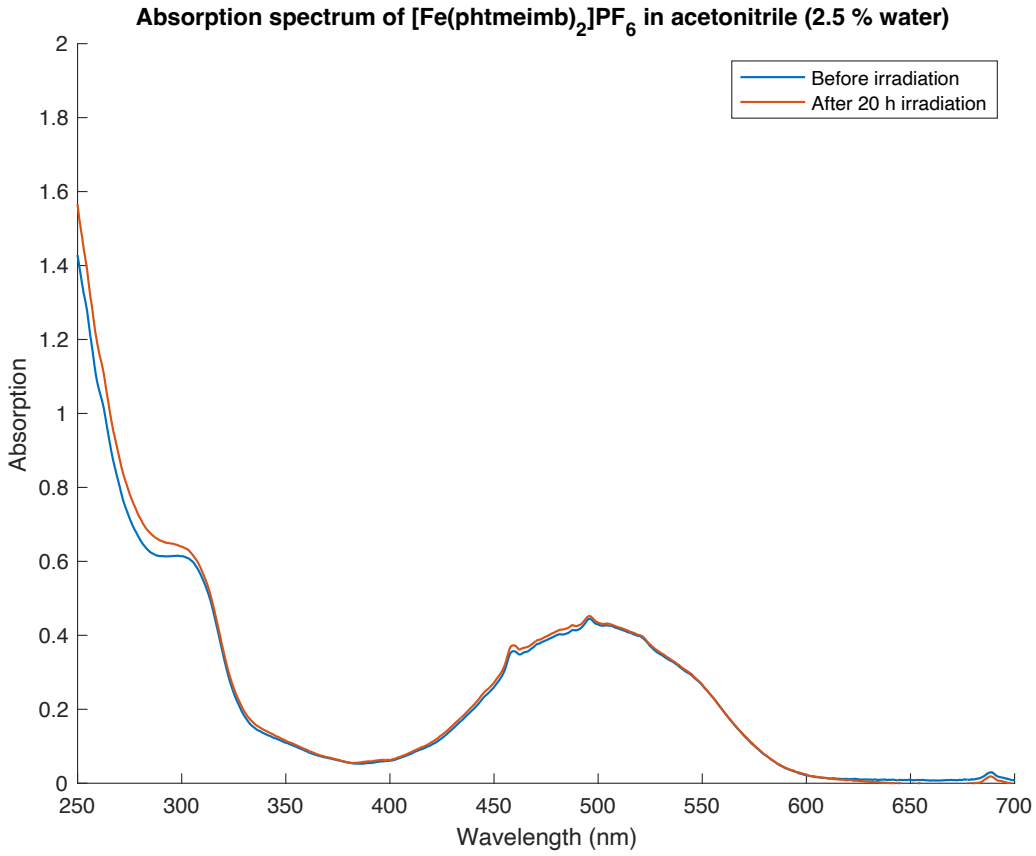

Figure S10. Absorption spectrum of $[Fe(phtmeimb)_2]PF_6$ (0.5 mM) in acetonitrile (2.5 % water), before and after irradiation for 20 h at λ = 530 nm, 3 W. The sample was diluted 1:3 before recording of absorption spectrum.

Cage Escape Yields

The concentration of electron transfer products after excitation with a ns laser flash were calculated using the transient absorption of the Fe(III)→Fe(II) reduction of $[Fe(phtmeimb)_2]^+$ ($\Delta\varepsilon$ = 9866 $M^{-1}cm^{-1}$ at 348 nm).[1] A solution of $[Ru(bpy)_3](PF_6)_2$ in acetonitrile matching the absorption of $[Fe(phtmeimb)_2]PF_6$ at the excitation wavelength was used as actinometer for the determination of the amount of absorbed photons based on the initial transient absorption of the ^{3}MLCT excited state ($\Delta\varepsilon$ = 11300 $M^{-1}cm^{-1}$ at 448 nm)[5] that is formed with unity quantum yield during the ns laser flash. From the ratio of reduced $[Fe(phtmeimb)_2]^+$ vs. excited $[Ru(bpy)_3]^{2+}$, together with a factor that accounts for any difference in absorbance between the sample and the actinometer, the quantum yield ϕ of electron transfer product is obtained. The latter is the product of the yield of excited state quenching η_q and the cage escape yield η_{ce} of quenching products that escape geminate recombination. Cage escape yields $\eta_{ce} = \phi/\eta_q$ were obtained from the quantum yield ϕ of the quenching products inferred from transient absorption spectroscopy as described above and the yield of excited state quenching η_q that was determined from the emission intensity ($\eta_q = 1 - (I/I_0)$) observed with the relevant quencher concentration.

Table S13. Determination of Cage Escape Yields

Quencher	$A_{Fe}(\lambda_{ex})$[a]	ΔA_{Fe} (348)[b]	Δ[Fe]/M [c]	$A_{Ru}(\lambda_{ex})$[d]	ΔA_{Ru}(452)[e]	Δ[Ru]/M[f]	f [g]	ϕ ([Q]/M)[h]	η_q[i]	η_{ce}[j]
Et_3N	0.51	0.0015	1.53 ×10^{-7}	0.52	-0.173	1.53 ×10^{-5}	1.01	0.010 (0.050)	0.44	0.02
TEOA	0.49	0.002	2.03 ×10^{-7}				1.03	0.012 (0.316)	0.47	0.03
$Co(dmgH)_2pyCl$	0.50	0 [k]	0				1.02	0 (0.015)	0.66	0

[a] Sample absorbance at the excitation wavelength (465 nm)
[b] Photo induced absorbance change of the sample at 348 nm
[c] Photo generated concentration of Fe(II) based on $\Delta\varepsilon$ = 9866 $M^{-1}cm^{-1}$ at 348 nm
[d] Actinometer absorbance at the excitation wavelength
[e] Photo induced absorbance change of the actinometer at 448 nm
[f] Photo generated concentration of $*[Ru(bpy)_3]^{2+}$ based on $\Delta\varepsilon$ = 11300 $M^{-1}cm^{-1}$ at 448 nm
[g] Correction factor for absorbance difference between sample and actinometer $f = \left(1 - 10^{-A_{Ru}(\lambda_{ex})}\right)/\left(1 - 10^{-A_{Fe}(\lambda_{ex})}\right)$
[h] Quantum yield of electron transfer products $\phi = (\Delta[Fe]/\Delta[Ru])f$
[i] Quenching yield from steady state emission quenching
[j] Cage escape yield $\eta_{ce} = \phi/\eta_q$
[k] No signal

References

1 K. S. Kjær, N. Kaul, O. Prakash, P. Chábera, N. W. Rosemann, A. Honarfar, O. Gordivska, L. A. Fredin, K.-E. Bergquist, L. Häggström, T. Ericsson, L. Lindh, A. Yartsev, S. Styring, P. Huang, J. Uhlig, J. Bendix, D. Strand, V. Sundström, P. Persson, R. Lomoth and K. Wärnmark, *Science (80-.).*, 2019, **363**, 249.

2 G. N. Schrauzer, G. W. Parshall and E. R. Wonchoba, in *Inorganic Syntheses*, ed. W. L. Jolly, 1968, vol. 11, p. 61–70.

3 B. D. McCarthy, D. J. Martin, E. S. Rountree, A. C. Ullman and J. L. Dempsey, *Inorg. Chem.*, 2014, **53**, 8350.

4 E. Brunner, *J. Chem. Eng. Data*, 1985, **30**, 269.

5 P. Müller and K. Brettel, *Photochem. Photobiol. Sci.*, 2012, **11**, 632.

6 S. P. Pitre, C. D. McTiernan, W. Vine, R. DiPucchio, M. Grenier and J. C. Scaiano, *Sci. Rep.*, 2015, **5**, 16397.